



Use of Time Series Analysis to Evaluate the Impacts of Underground Mining on the Hydraulic Properties of Groundwater of Dysart Woods, Ohio

Qian Zhang¹ · Dina L. López²

Received: 28 January 2018 / Accepted: 24 July 2019 / Published online: 2 August 2019
© Springer-Verlag GmbH Germany, part of Springer Nature 2019

Abstract

Dysart Woods is the largest (≈ 23 ha) old-growth forest in southeastern Ohio. It was donated to Ohio University for research purpose and public use by the Nature Conservancy. The mineral rights beneath Dysart Woods are held by the Ohio Valley Coal Company, who conducted underground coal mining in the area. We performed correlation analyses of time series data of precipitation, hydraulic head, barometric pressure, and Earth tide data from before and after mining to characterize the hydrogeologic processes and changes in the aquifers in the mined areas. Results of transient data analyses revealed higher permeability and hydraulic conductivity after mining and decreased storage capacity in the upper groundwater system. Analysis of the Earth tide data also suggested that the groundwater flow regime responded better to Earth tides prior to mining than after mining, which was probably due to the draining of water through mining-induced fractures in the system. Changes in hydrogeologic parameters suggest that the capacity of aquifers to hold water against gravity has declined, due to increased fracturing and faster vertical movement of water. At Dysart Woods, old trees obtain water from springs that discharge groundwater. If the groundwater levels drop, the Dysart Woods ecosystem can be adversely affected. Increased understanding of the potential hydrogeologic impacts of longwall mining subsidence is necessary, especially for mine operators and regulators, to preserve the ecosystems that rely on the groundwater flow system. In addition, it is very important that mine operator and regulators cooperate, as it is not enough to protect the soil surface from subsidence; the surface and groundwater systems should also be preserved.

Keywords Time series analysis · Correlation · Earth tide · Groundwater flow · Hydrogeological properties

Introduction

Coal, one of the primary energy sources for generating electricity in the U.S., has been mined in the state of Ohio since the 1800s. Underground mining accounts for approximately 60% of Ohio coal production (ODNR 2005).

The environmental impacts of longwall mining are well documented, and include surface subsidence, loss of water resources, alterations in hydraulic properties of mined areas,

changes in the overburden stress regime, and addition of flow pathways (Altun et al. 2010; Booth 2002, 2006; Hasenfus et al. 1988; Karacan and Goodman 2009; Kendorski 1993; Kim et al. 1997; Liu et al. 1997; Marschalko et al. 2012; Sahu et al. 2009; Singh et al. 2008; Stoner 1983). Here we focus on two major impacts: subsidence and changes in hydraulic properties.

As depicted in Fig. 1, surface subsidence is greatest over the center of the extracted panel. The lateral distance from the boundaries of the longwall mine to the point of zero subsidence is determined by the “angle of influence”, which is used to calculate the “buffer zones” intended to preserve surface structures (Bell and Genske 2001). In the northern Appalachian Plateau areas, the average angle of influence was set to be $30^\circ \pm 10^\circ$ (Ground Water Associates 1991). The angles of influence at Dysart Woods were reported between 13° and 49° (OVCC 2003; Marino 2003), and the corresponding buffer zones ranged from approximately

✉ Qian Zhang
qzhang@gradientcorp.com; zhang92.qz@gmail.com

Dina L. López
lopezd@ohio.edu

¹ Gradient, 20 University Road, Cambridge, MA 02138, USA

² Department of Geological Sciences, Ohio University, Athens, OH 45701, USA

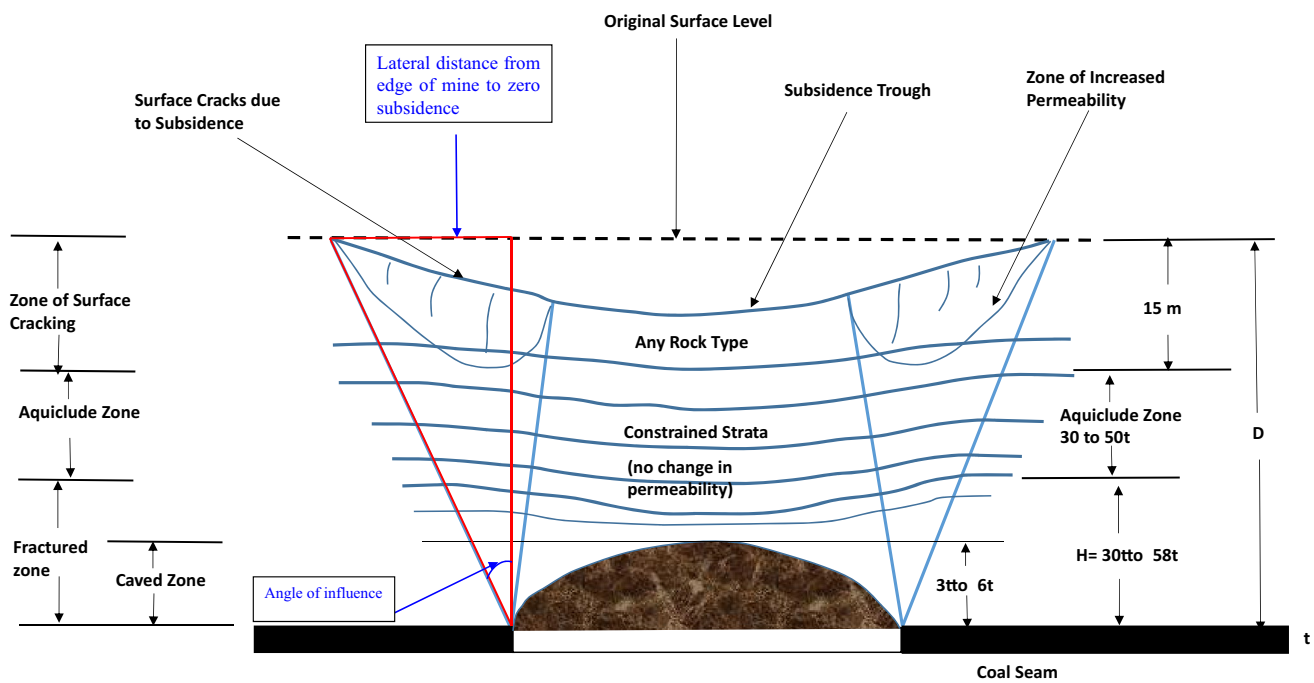


Fig. 1 Subsided zones above a longwall mining area (modified from Booth 2002; Singh and Kendorski 1981): t represents “the height of the extracted coal”; H represents “the thickness of the fractured zone”, and D represents “the height of the aquiclude”

90–213 m (300–700 ft). However, these angles of influence and buffer zones are used to protect surface structures, and no consideration was given to groundwater resources.

Booth (2002) divided the subsided overburden into four zones: the caved zone, the fractured zone, the aquiclude zone or zone of continuous deformation, and the zone of surface cracking (Fig. 1). The caved zone normally extends 2–8 times the thickness of the coal seam, and includes the overburden materials that collapse into the mined area. The fractured zone typically extends 30–40 times the height of the coal seam; the fractures extend both vertically and horizontally. The aquiclude zone is a continuous deformation zone that lies on top of the fractured zone, extending approximately 15 m (50 ft) below the ground surface. The aquiclude zone usually bends or deforms without extensive breaking. The zone of surface cracking is a near-surface fractured zone caused by tensional stresses on the margins above the longwall mining area within the buffer zone (Booth 2002).

After mining, the higher secondary permeability created by mining increases the rate of flow through the overburden. If there is not sufficient inflow from precipitation to compensate for the increased hydraulic conductivity, the upper shallower aquifers will be drained, thus reducing spring discharges and lowering water levels. Changes in groundwater hydrology can also adversely affect forest ecosystems, because decreases in groundwater levels reduce discharges at springs that are water sources for the forest (Burgess 2006). Stoner (1983) found that the groundwater flow system at a

historic mining site was controlled by mining induced fractures (e.g. secondary permeability), and that the observed water-level decline was also caused by mining. Kim et al. (1997) applied a finite element poroelastic model to evaluate mining-induced strata failure and showed that changes in water content, flow direction, and hydraulic conductivity were associated with longwall mining.

Researchers have proposed various protective mechanisms to reduce the impacts of underground mining. For example, Bell and Genske (2001) defined buffer zones to preserve surface structures based on the angle of influence. However, depending on the defined angle, this may only protect surface structures from subsidence and will not preserve hydrogeologic properties. Fan and Zhang (2015) reported that several crucial factors are important to protect groundwater supply: movement of key strata (strata that control overburden movement), appropriate interburden thickness, and protection of the aquiclude immediately below the aquifer. Based on their study, as long as key strata remain intact (not broken or collapsed), the overlying aquifer or aquiclude can be preserved.

The purpose of this study was to demonstrate that transient data analysis combined with flow modeling studies (Cook 2008) can provide useful information about current and future hydrogeology of a region affected by mining activities. We analyzed pre and post-mining hydraulic conditions using data collected before and after underground mining in three well nests that recorded well heads during

the study period. Hourly data for precipitation were collected from the Belmont County Wheeling Airport Station (Cook 2008; Zhang 2010). We used time series analysis to quantify the impacts of subsurface mining on the unsaturated zone and upper aquifers. The changes in hydrogeological properties (e.g. hydraulic heads, aquifer permeability, storage capacity) and hydrological responses to Earth tides before and after mining were characterized and compared to provide a better understanding of the local groundwater system and how it has been affected by mining.

Study Area

Overview of Dysart Woods

Dysart Woods is the largest old-growth forest (≈ 23 ha) in southeastern Ohio, with trees older than 400 years (McCarthy et al. 2001). It is located in a never-glaciated portion of the Allegheny Plateau in Belmont County, which is a major coal producer in Ohio. Dysart Woods has been designated as a National Natural Landmark by the U.S. Department of the Interior (National Park Service 2004). Dysart Woods is also an outdoor laboratory of Ohio University. The surface rights of Dysart Woods belong to Ohio University under an agreement to manage the land in its natural condition (Burgess 2006), while the mineral rights are held by the Ohio Valley Coal Company (OVCC), which conducted underground mining to exploit the coal in this area. There are five major coal beds in Belmont County: the Pittsburgh (no. 8), Meigs Creek (no. 9), Uniontown (no. 10), Waynesburg (no. 11), and Washington (no. 12). The Pittsburgh #8 Coal Seam has been mined by OVCC at Dysart Woods (Fig. 2). This coal bed is almost 2 m thick and is found at depths between 100 and 177 m (330–580 ft) below the ground surface (Marino 2003).

Conflicts have existed between OVCC and local environmental groups for decades. The latter have argued that fracturing and subsidence from mining will modify shallow drainage and reduce the groundwater supply to the forest (Booth 2006). The general mining extent at Dysart Woods is shown in Fig. 2. Light blue represents room-and-pillar mining, which passess directly beneath Dysart Woods from southeast to northwest. To prevent subsidence within the old growth forest areas, the room-and-pillar mining there has a maximum extraction ratio of 50%, compared to a ratio of 65% outside of the forest area. Longwall mining (in pink) operations were conducted within the Dysart Woods watershed.

There are a total of eight groundwater monitoring wells grouped into three well nests (WN1, WN2, WN3, Fig. 2) in Dysart Woods that were drilled in 2005 prior to the exploitation of the coal. WN1 was installed over the longwall mining

area, (GW-6, GW-7, and GW-8); WN2 was placed over the room-and-pillar mine (GW-3, GW-4, and GW-5); while WN 3 was positioned over a non-mined area (GW-1 and GW-2).

Local Hydrogeology

Belmont County has a continental climate. The average annual precipitation is the area is ≈ 107 cm (42 in.), and potential evapotranspiration is ≈ 63.5 cm (25 in.) (Holt and Craig 1997). Precipitation is the only source of recharge to groundwater in the study area (Anderson 2001); recharge varies from 11 to 19 cm (4.2 to 7.6 in) per year (Ground Water Associates 1991). The most common water-bearing lithologies at Dysart Woods include sandstone, limestone, siltstone, coal, and unconsolidated material (Anderson 2001). Shallow aquifer systems in Dysart Woods are bounded by local dissected topography, which limits the lateral extent of these aquifers. Groundwater divides for these shallow aquifers are often determined by the watershed drainage areas (Ground Water Associates 1991).

Previous Studies of Dysart Woods

There are a few studies about the hydrogeological properties and mining impacts at Dywart Woods. Schillig (2005) described the installation of the eight monitoring wells to collect hourly water level data (Fig. 2). Slug tests were conducted to determine the pre-mining hydraulic conductivity. The results confirmed the existence of shallow groundwater systems (perched aquifers), which are the likely sources of springs in the area. The author suggested that subsidence could disrupt the discharge of springs and seeps that were fed by the perched aquifers.

Cook (2006) studied the impacts of longwall mining at Dysart Woods on the water systems by comparing pre- and post-mining aquifer properties. The results suggested that longwall mining could increase the hydraulic conductivity of shallow perched aquifers. Also, hydraulic head loss was confirmed, which could occur as soon as 1 week after the longwall mining passed beneath the impacted wells. Cook (2008) further evaluated the hydrogeologic impacts on the watershed by developing physical models of the groundwater system for pre- and post-mining situations. Numerical modeling was conducted using MODFLOW, which indicated that the hydraulic heads of the shallowest aquifer at the northeastern portion of the studied area would drop after longwall mining. Transient numerical models also showed that the upper hydrostratigraphic units would dry up due to subsurface mining (simulation period 2004–2008). Forest vegetation would be adversely impacted if perched aquifers dry up and do not recover. Therefore, the author proposed that new regulations should be enacted based on watershed boundaries in order to preserve ecosystems.

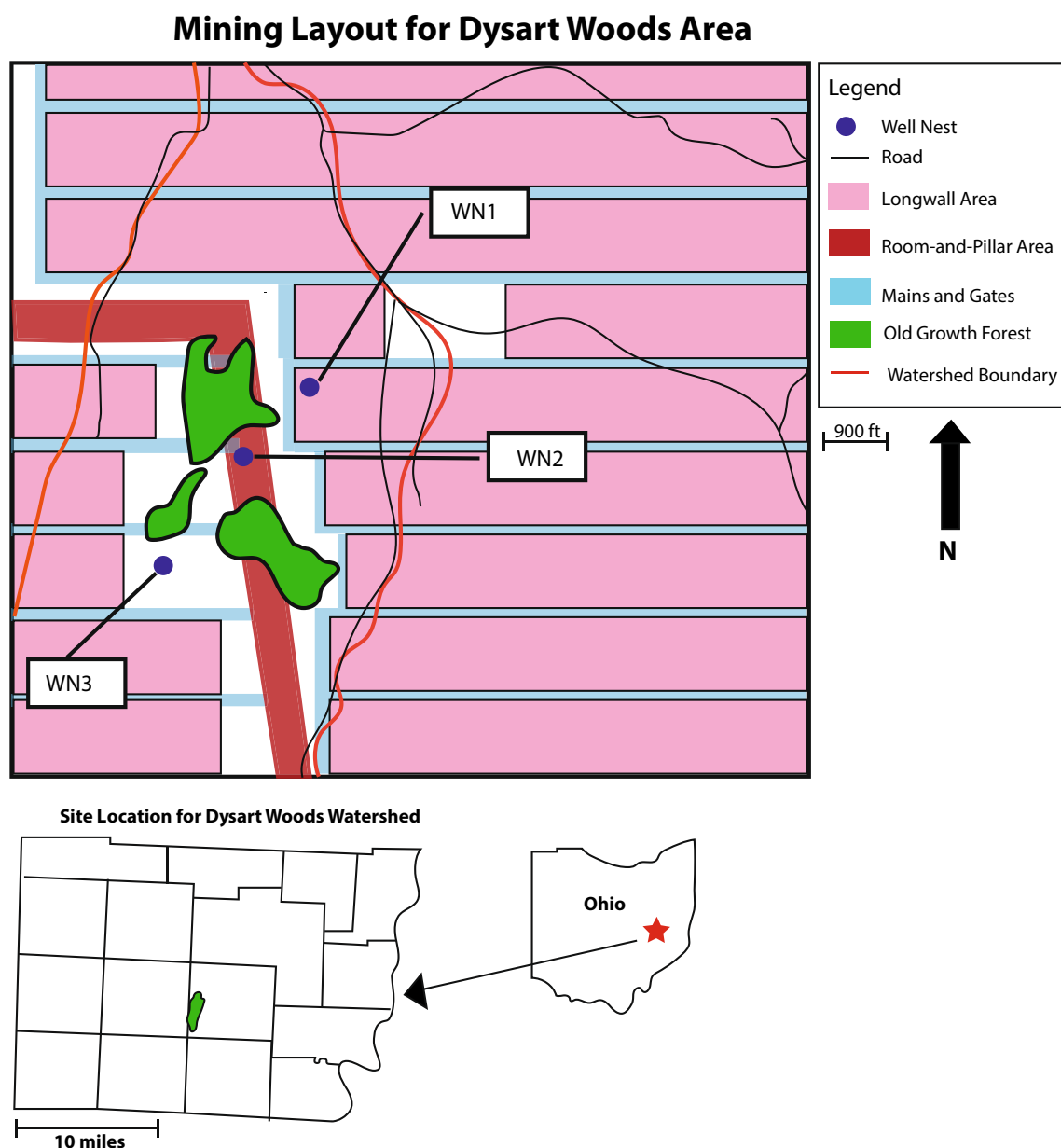


Fig. 2 Location, mining extents, monitoring wells, and watershed boundary at Dysart Woods (after Cook 2008)

Burgess (2006) studied the effects of mining-related changes in hydrology on the Dysart Woods forest ecosystem and found that plants up- and downslope of the springs were using groundwater, especially during the growing season and during droughts. The author proposed that groundwater was important to the biogeochemistry of Dysart Woods and that hydrologic changes could adversely impact forest ecosystems.

Methodology

Descriptions of Time Series Analyses

A time series is defined as a set of sequential values of a variable produced in time or measured sequentially in time (Box and Jenkins 1976; Chatfield 1980), such

as recharge/discharge, hydraulic head data, varved lake sediments, seismic data, growth lines on fossils, sequence of bed thickness, etc. Time series applications are widely used in modeling complex water resource problems, especially in fractured and karstic systems (Bernard and Delay 2008; Crosbie et al. 2005; Healy and Cook 2002; Kim et al. 2000; Larocque et al. 1998; Lee and Lee 2000; Manga 1999) as well as in mined areas (Sahu et al. 2009). For example, Larocque et al. (1998) applied time series analysis to identify spatial–temporal characteristics and hydrologic processes in a karst aquifer, including specific yield, storage, and drainage potential. This study demonstrated that correlation and spectral analyses could contribute significantly to the regional study of a large karst aquifer. Lee and Lee (2000) conducted a time series analysis using correlation and spectral analysis to investigate the hydrogeologic processes in a fractured aquifer. Their results indicated that time series analysis provided reliable results because the parameters computed from the time series data (time delay, specific storage, and porosity) were consistent with tracer tests at study sites. Bernard and Delay (2008) applied time series analyses to investigate the relationship between barometric pressure, Earth tide, and hydraulic head variations in a confined calcareous aquifer. They calculated specific storage and porosity of the aquifer using time series data and compared these parameters with field measurements. The results supported that storage coefficient and specific yield values could be accurately estimated using time-series analyses, while calculated porosity was underestimated. Sahu et al. (2009) used time series analysis to better understand the characteristics and processes controlling flow at an abandoned mine site.

Depending on the number of variables, time series analysis can include one-variable (univariate) analysis and multivariate analysis. Tables 1 and 2 briefly summarize the definitions and applications of one-variable analysis and two-variable analysis. One-variable analysis describes each individual structure of the time series. The functions used in the analysis include auto-correlation (in the time domain) and the simple spectral analysis (in the frequency domain). Two-variable analysis characterizes the transformation of the input signal (e.g. precipitation, Earth tides) into the

output signal (hydraulic heads), and therefore indicates the correlation between input and output. The cross-correlation function is applied in the time domain, while cross-spectral analysis, cross-amplitude, phase, coherence and gain functions are applied in the frequency domain. For auto-correlation analysis, the variable is shifted in time and the correlation coefficient between the shifted variable and the original variable is found for every lag. In a similar way for cross-correlation, the second variable (output) differs from the first (input). Transformation of the variables from the time to the frequency domain allows calculation of the spectrum frequencies of the variables. The mathematical details of the functions used in our study are described in Sahu et al. (2009) and the equations are summarized in “Appendix 1”. A FORTRAN computer program based on the “Appendix 1” equations was used for the calculations.

Estimation of Specific Storage and Porosity

In a confined aquifer, specific storage (S_s) and total porosity (n) can be estimated using time series data analysis (Marine 1975; Larocque et al. 1998; Lee and Lee 2000; Bernard and Delay 2008). Earth tides are related to the dilation of a confined aquifer and produce groundwater level fluctuations (Bredehoeft 1967), which can be used to calculate specific storage:

$$S_s = \frac{\theta}{\Delta h} \quad (1)$$

where θ is the theoretical tidal strain dilation ($\theta = 4.5 \times 10^{-8}$) and Δh is the changes in hourly piezometric heads (semi-diurnal, 12 h).

Jacob (1940) proposed the following formula to relate storage coefficient (S_s) and porosity (n) through a constant (B), which reflects the barometric fluctuations observed in a confined aquifer with the daily variations in atmospheric pressure:

$$n = \frac{E_w B S_s}{\rho g} \quad (2)$$

where E_w is the elasticity module of water ($2.1 \times 10^9 \text{ kg m}^{-1} \text{ s}^{-2}$), ρ is the water density (999 kg m^{-3}),

Table 1 Summary of parameters and approach of one-variable analysis

Input	Precipitation	Hydraulic head
Output	Precipitation	Hydraulic head
Auto-correlation (simple correlation)	To determine the relationships within the consecutive data points and information about the periodicity and memory effect. Correlograms are plotted for the autocorrelation $r(k)$ against time lag k . The slope of correlogram decreases dramatically when there is an event with a short memory effect; and decreases slowly during a long-term memory effect	
References	Chatfield (2000); Kendall and Ord (1990); Larocque et al. (1998); Lee and Lee (2000); Sahu et al. (2009)	

Table 2 Summary of parameters and approach of two-variable analysis

Input	Precipitation	Earth tides
Output	Hydraulic heads	Hydraulic heads
Cross correlation	To establish the cross-relationship between the input and output series; $r_{xy}(k)$ is the cross-correlation function. The plot of $r_{xy}(k)$ against lag k is called the cross-correlogram. In cross-correlogram, the time lag between zero and maximum $r_{xy}(k)$ is called delay, which suggests how stresses propagate through the groundwater system. The shorter the delay, the faster it travels through the system	The plot of $r_{xy}(k)$ against lag k is called the cross-correlogram, which suggests how stresses propagate through the groundwater system
Cross spectral analysis	It is the correlation function transformed into frequency components. It determines the relationship between two time series as a function of frequency, <i>e.g.</i> , how closely the two variables are correlated at each frequency	It determines the relationship between two time series as a function of frequency, <i>e.g.</i> , how closely the two variables are correlated at each frequency
Cross-amplitude	Identifies how the input signal has been changed through the system and transformed into the output signal. It determines the filtering characteristic of the system on periodic components of the input stresses	Identifies how the input signal has been changed through the system and transformed into the output signal. It determines the filtering characteristic of the system on periodic components of the input stresses
Coherence	Shows the relationship between the two time series in terms of frequency, which indicates if changes in the output series correspond to the same type of changes in the input series. It determines if the variability of two distinct time series is interrelated in the spectral domain	Shows the relationship between the two time series in terms of frequency, which indicates if changes in the output series correspond to the same type of changes in the input series. It determines if the variability of two distinct time series is interrelated in the spectral domain
Gain	Shows the attenuation or amplification of amplitude of the output signal compared with the input signal. Attenuation occurs when the gain function value is less than 1. A value of the gain function larger than 1 means an amplification	Shows the attenuation or amplification of amplitude of the output signal compared with the input signal. Attenuation occurs when the gain function value is less than 1. A value of the gain function larger than 1 means an amplification
References	Box and Jenkins (1976); Chatfield (2000); Larocque et al. (1998); Padilla and Pulida-Bosch (1995); Sahu et al. (2009)	

Table 3 Surface and bottom elevations of groundwater monitoring wells

Well ID	Surface elevation (m)	Depth to bottom (m)	Elevation at bottom (m)	Depth to top of no. 8 coal (m)
<i>Well Nest 1</i>				
GW-8	395	22.6	372.1	166.1
GW-7	395	15.5	379.2	166.1
GW-6	395	7.5	387.2	166.1
<i>Well Nest 2</i>				
GW-5	402	47.1	355.2	173.7
GW-4	402	8.2	394.1	173.7
GW-3	402	20.1	381.3	173.7
<i>Well Nest 3</i>				
GW-2 (dry)	402	26.1	376.3	184
GW-1 (dry)	402	9.1	393.2	184

Elevation of Pittsburgh #8 coal seam is about 228 m (750 ft) above sea level (Ground Water Associates, Inc 1991)

and g is the acceleration of gravity (9.81 m s^{-2}). B is the barometric efficiency coefficient, and can be calculated using the gain function at the frequency corresponding to the daily barometric variation (24 h).

Data Collection

Tidal pressure is one of the common and continuous forces that affect groundwater levels (Freeze and Cherry 1979). It is the combined effect of gravitational interaction between the Earth, Sun, and Moon, including diurnal and semi-diurnal constituents. According to Rojstaczer and Agnew (1989), dilation and compression occur during the daily tidal cycle. When an aquifer compresses, hydrostatic pressure increases, which causes water level in boreholes to rise. By contrast, when rock dilates, the pressure decreases and the water levels drop in boreholes. Earth tide data are often used to characterize aquifer hydraulic properties. For example, Heish et al. (1987) used transient analysis to determine how an artesian aquifer responds to pressure head disturbance caused by Earth tide dilatation of the aquifer and Léonardi and Gavrilenko (2003) estimated the strain sensitivity of a well, aquifer conductivity, specific storage, and its degree of confinement using Earth tide analysis.

Data used in our current time series analysis were obtained from three sources: (1) Hourly precipitation data of Belmont County were purchased from weather-warehouse.com. (2) Hourly hydraulic heads were collected from the groundwater monitoring wells (Fig. 2), including GW-6 and GW-7 in WN 1 and GW-3, GW-4, and GW-5 in WN2. Wells in WN3 were not used because these wells were screened above the water table during the monitoring period. Detailed information about these monitoring wells is listed in Table 3.

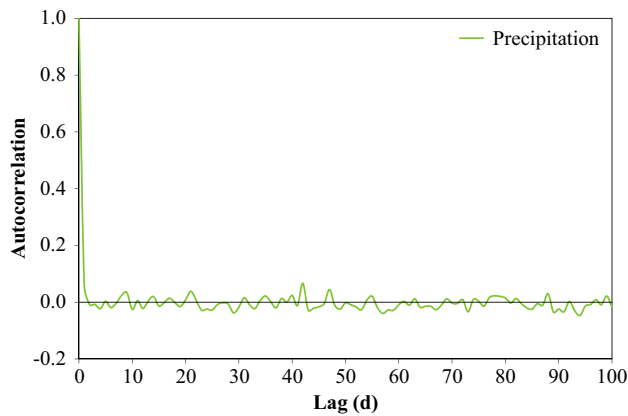


Fig. 3 Autocorrelation functions for precipitation time series from September to December 2009. Note the autocorrelation function drops rapidly to 0 after about 3 days

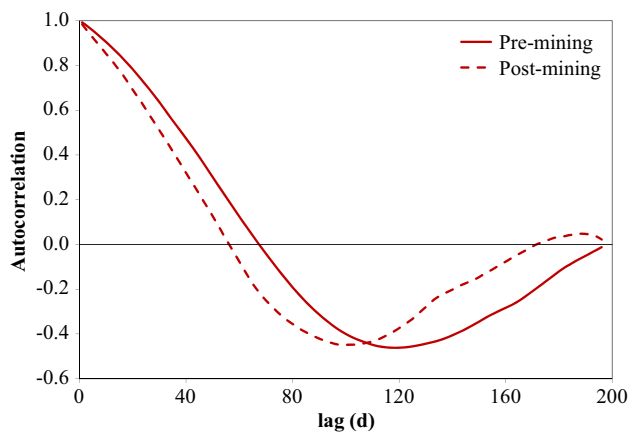


Fig. 4 Autocorrelation functions for hydraulic head time series in GW-3. The autocorrelation of post-mining hydraulic heads (dashed line) decreased faster than pre-mining conditions

(3) On-site Earth tide potentials during the monitoring period were calculated based on the well location coordinates. The program ETGTAB was used to calculate the Earth tides (Wenzel 1996).

Results and Discussion

Auto-correlation

The auto-correlogram of precipitation data displayed a quick initial damping with small oscillation along with an increased time lag, showing a short memory effect (Fig. 3). The correlation was very low after approximately 3 days, indicating independence between different rainfall events, i.e. there was no correlation between two consecutive events after a few lags.

Autocorrelation of daily hydraulic heads was calculated to compare changes between pre- and post-mining periods. Figure 4 shows the autocorrelation functions for GW-3. It was noticed that the hydraulic head autocorrelation function had a longer delay (time decrease to zero) for pre-mining conditions (≈ 67 days) than for post-mining conditions (≈ 56 days). In general, the faster the autocorrelation coefficient decreases with time, the shorter the influence of the particular event on the system. This behavior suggests that changes in hydraulic head occurred quicker after mining, which were probably due to increased hydraulic conductivity and flow velocities.

Cross-correlation of Daily Data

Continuous data series were selected at equal time intervals of different years for the entire monitoring period to compare changes between the pre and post-mining conditions. Daily precipitation and hydraulic head data were averaged from the hourly records. In the cross-correlation analysis, precipitation or Earth tide data were used as input signals and hydraulic heads were the output series. As pointed out by Larocque et al. (1998), hydraulic heads are affected by precipitation as well as Earth tides and can provide information on the state of the aquifer system.

Time Series of Daily Precipitation and Hydraulic Heads

Cross-correlation was conducted using daily precipitation as input and hydraulic heads as output data to investigate the characteristic relationship between rainfall events and the corresponding groundwater levels. The results of GW-6 and GW-7 are plotted in Figs. 5a, b and 6a, b to compare the changes from pre-mining state to post-mining state. The delay, which is defined as the time lag between zero and the maximum cross-correlation coefficient ($r_{xy}(k)$), gives information on how the input signal propagates through the system. Normally, a longer delay represents precipitation traveling slowly through the unsaturated zone, while a shorter delay suggests a faster travel velocity (Larocque et al. 1998). Similarly, small $r_{xy}(k)$ indicates reduced/weak signal between the input and output data series.

As we can see from Fig. 5, the delay of GW-6 during the pre-mining period was approximately 8 days with a maximum cross-correlation coefficient of 0.114; the delay for the post-mining period decreased to 2 days with an increased cross-correlation coefficient of 0.22. The responses of GW-7 were similar: the delay was 5 days with $r_{xy}(k)$ value of 0.03 before mining, whereas the delay dropped to 2 days with an increased $r_{xy}(k)$ of 0.08. The shortened post-mining delays indicated that precipitation rapidly infiltrated the soils and moved into the saturated zone of the mine (Lee and Lee 2000). Moreover, higher $r_{xy}(k)$ values for post-mining

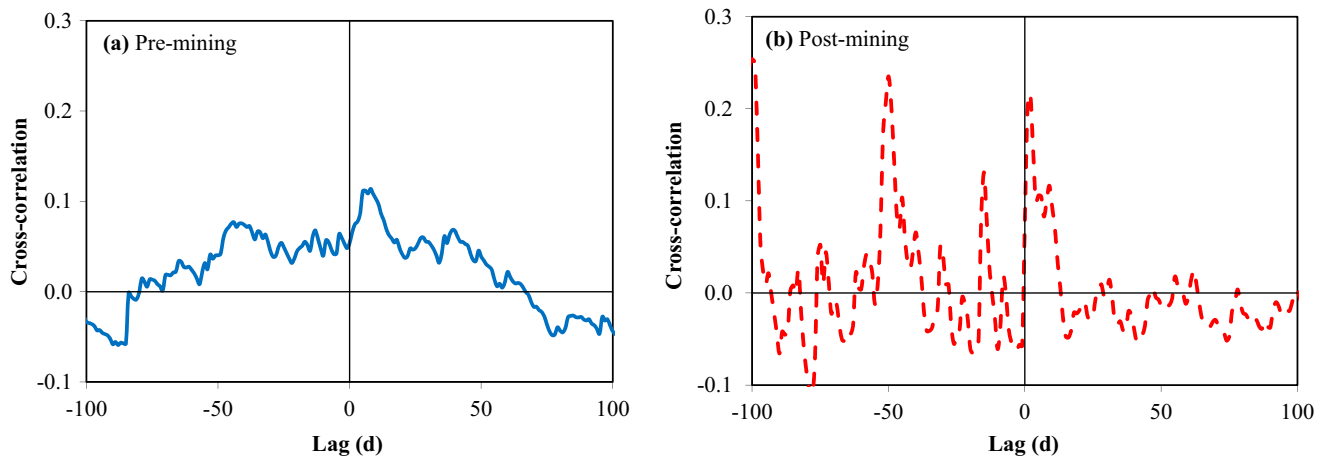


Fig. 5 Cross-correlations for daily precipitation and hydraulic head times series of GW-6 for **a** pre-mining; and **b** post-mining conditions. Note that the maximum $r_{xy}(k)$ was much lower, and the delay was longer in the pre-mining situation

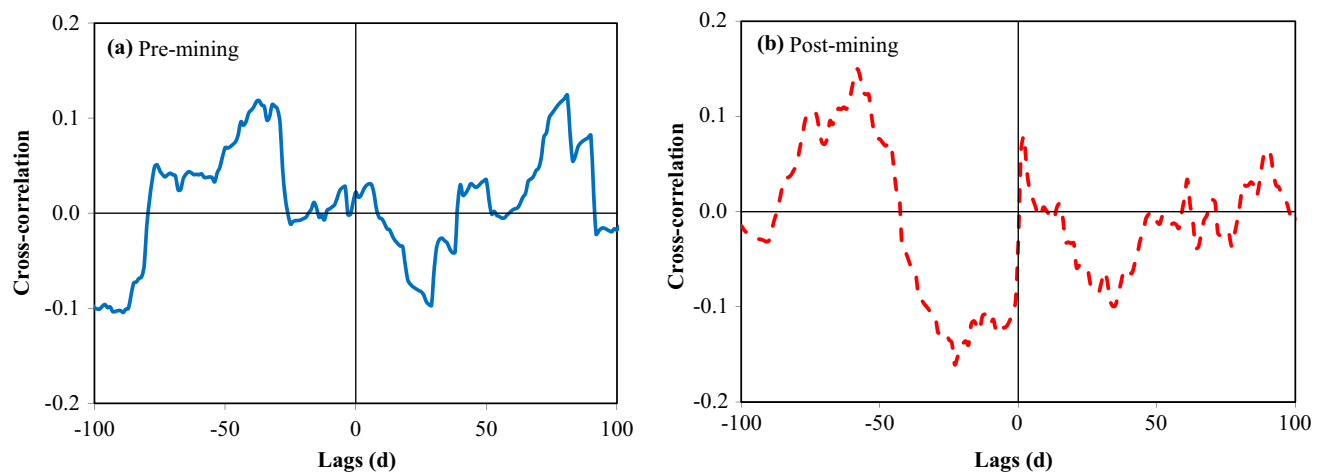


Fig. 6 Cross-correlations for daily precipitation and hydraulic head times series of GW-7 for **a** pre-mining; and **b** post-mining conditions. Note that the maximum $r_{xy}(k)$ was much lower, and the delay was longer in the pre-mining situation

conditions suggests an increase in the signal transfer between rainfall and hydraulic heads, and that water level in the wells were influenced by rainfall more directly. Note that GW-6 and GW-7 were both located directly above the longwall mining; therefore, the quicker response was likely caused by the higher hydraulic conductivity created by mining. According to Fetter (2001), hydraulic conductivity can be increased by several orders of magnitude by subsidence (or rock fracturing). Vertical hydraulic conductivity were also increased as perched aquifers were fractured, which decreased the groundwater residence time in the shallowest perched aquifer. These results indicate that longwall mining changed the hydrologic properties of the mined area, such as permeability, storage, discharge, and groundwater residence time, probably due to rock fracturing. The relative low values of the cross-correlation coefficient for pre- and

post-mining data were probably caused by the different travel paths that water was able to follow in a porous or fractured system.

Cross-correlation of Daily Hydraulic Heads Among Different Wells

Cross-correlation analysis was performed between the hydraulic heads of two different wells at selected periods of time when continuous data were available. The input time series was the shallower wells (GW-6 and GW-7) and the output data series was the deeper one (GW-8). The results are plotted in Figs. 7 and 8, respectively.

As Figs. 7a and 8a show, cross-correlation coefficients were positive between GW-6 versus GW-8 and

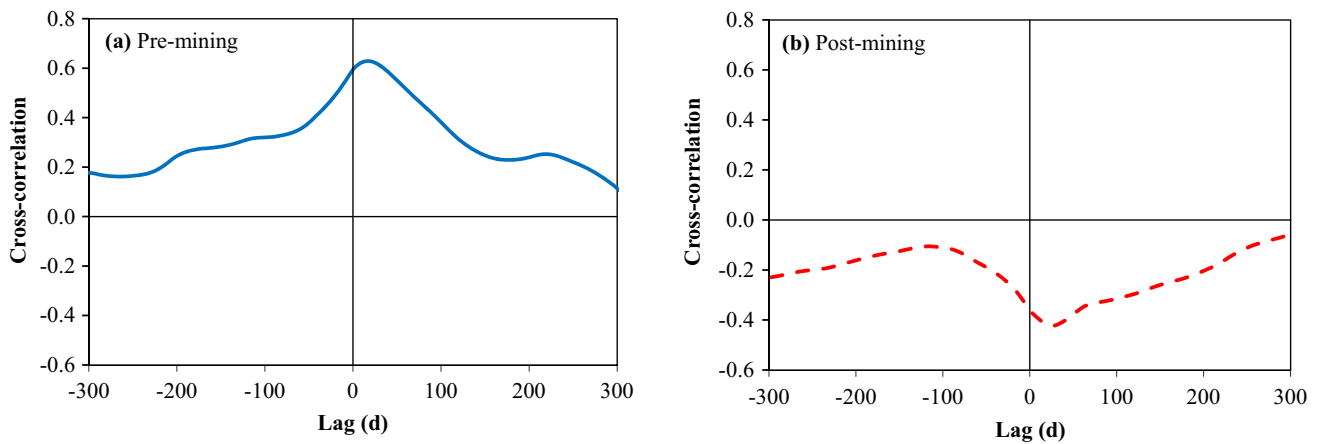


Fig. 7 Cross-correlations for daily hydraulic heads of GW-6 and GW-8 **a** pre-mining, and **b** post-mining

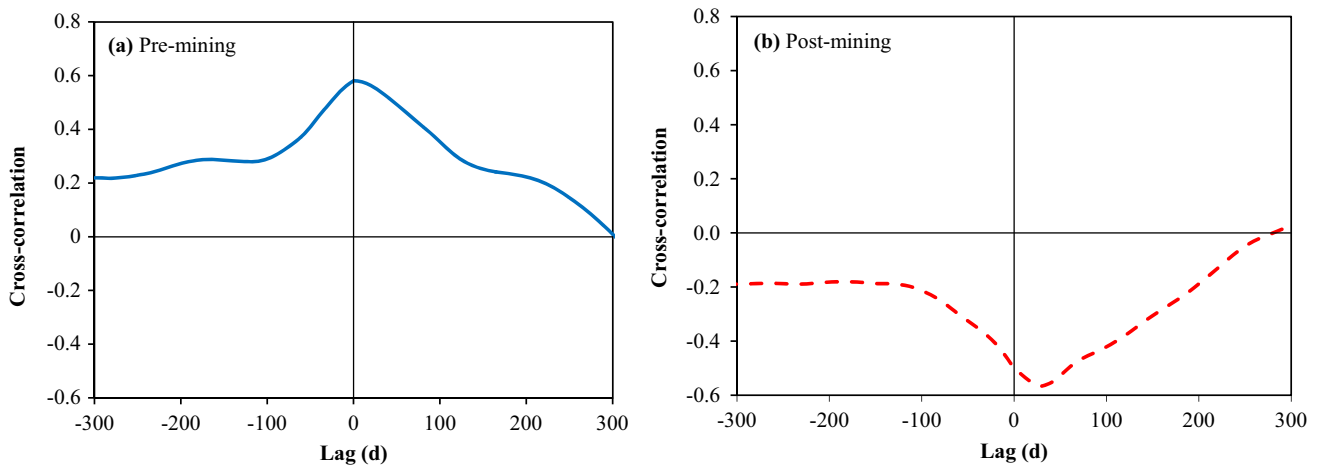


Fig. 8 Cross-correlations for daily hydraulic heads of GW-7 and GW-8 **a** pre-mining, and **b** post-mining

GW-7 versus GW-8 prior to mining, with a maximum value of 0.63 and 0.58, respectively. The positive lags identified at maximum $r_{xy}(k)$ are the time periods for a head perturbation signal in the shallower well traveling to the deeper well. The graphs (Figs. 7b, 8b) showed an opposite behavior with respect to the cross-correlation for post-mining conditions, where cross-correlations become negative: -0.42 for GW-6 versus GW-8, and -0.57 for GW-7 versus GW-8. The negative minimum $r_{xy}(k)$ in the cross-correlation suggests that the hydraulic heads in the deeper well responded differently than the shallower well; water levels in the deeper well declined as the input signal dissipated. The negative cross-correlations in both Figs. 7b and 8b were caused by GW-8 (the deeper well) losing water to the mining area beneath, even though the

shallower wells (GW-6 and GW-7) had rising water levels from rainfall.

Cross-correlation of Hourly Data

Because precipitation in Ohio is usually not evenly distributed, the impacts of a precipitation event may still affect the groundwater level when a subsequent precipitation event takes place shortly after the first one. It is also highly possible that there are multiple flows generated due to the different infiltration rates associated with various lithologies. To evaluate the changes associated with mining without the impacts of multiple precipitation events, we picked out several short-term (no more than a week) precipitation events that took place with no obvious rainfall before and after the selected events.

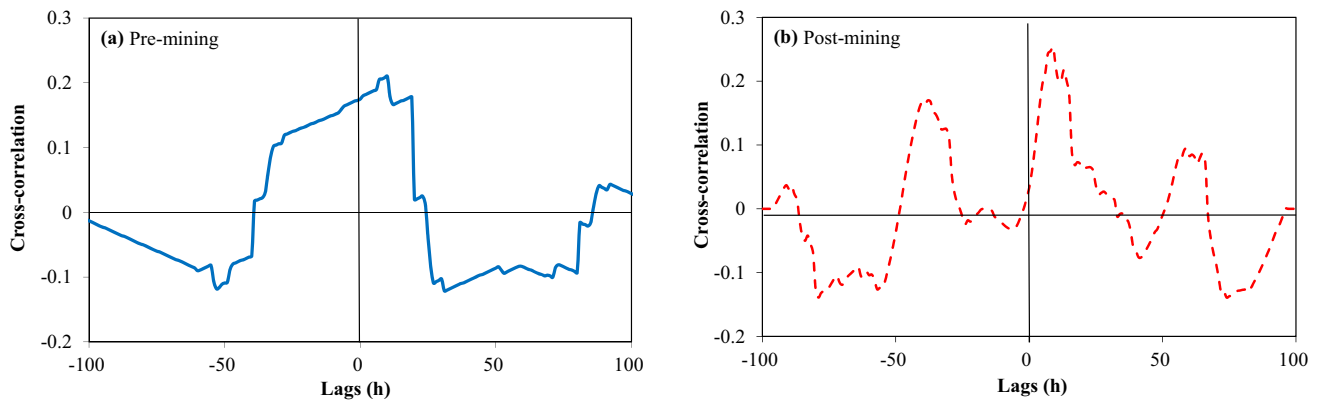


Fig. 9 Cross-correlations for hourly hydraulic heads of GW-7 **a** pre-mining, and **b** post-mining

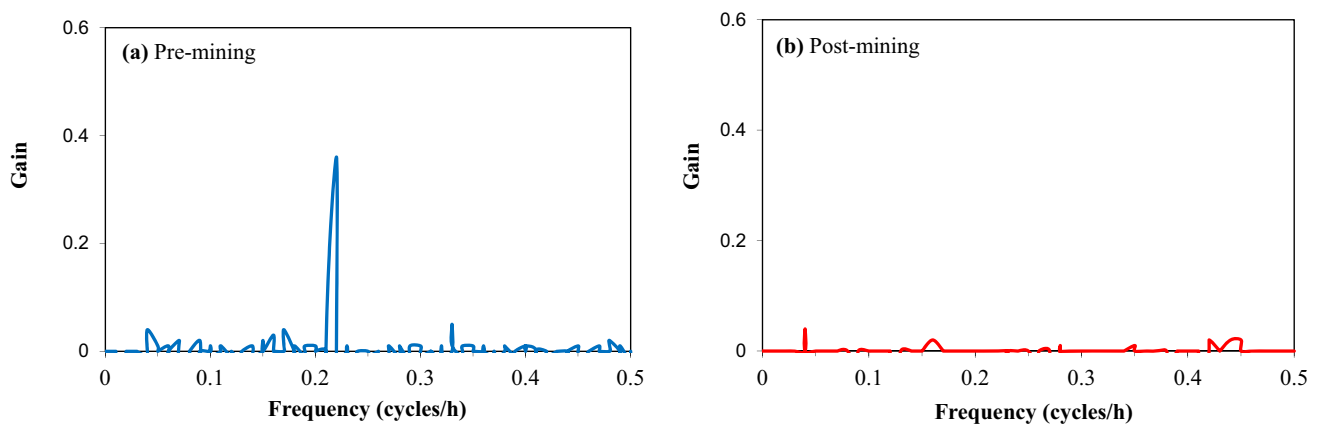


Fig. 10 Gain functions for hourly precipitation and hydraulic head of GW-7 **a** pre-mining, and **b** post-mining

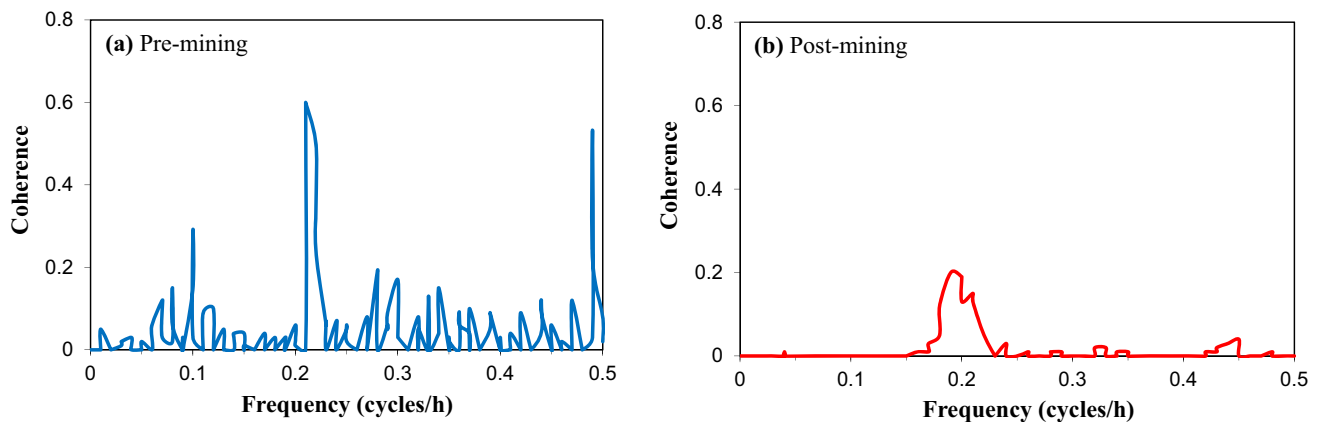


Fig. 11 Coherence functions for hourly precipitation and hydraulic head of GW-7 **a** pre-mining, and **b** post-mining

Cross-correlation Between One Precipitation Event and Hydraulic Head

Cross-correlation and cross-spectral analyses were conducted using hourly precipitation data as input; hydraulic

heads in GW-7 were used as output data. The results of cross-correlation, gain, and coherence for pre- and post-mining are presented in Figs. 9, 10, and 11, respectively. Figure 9a shows that the delay time between precipitation and hydraulic head response was 10 h, with a maximum

cross-correlation coefficient of 0.21 for pre-mining conditions. The delay decreased to about 8 h, with a maximum coefficient of 0.25 for post-mining conditions (Fig. 9b). The shorter delay indicates input signal (precipitation) is transferred faster through the system after mining, which is consistent with the results in daily cross-correlation analysis (Figs. 5, 6).

Gain function can be used to investigate the filtering or amplification characteristics of a system. In a time series analysis, Padilla and Pulido-Bosch (1995) suggested that a gain coefficient greater than 1 indicates “baseflow,” a gain coefficient value between 1 and 0.4 means “intermediate flow,” and values less than 0.4 correspond to “quick flow”. As shown in Fig. 10, the gain function has a higher value (≈ 0.40) for pre-mining conditions than post-mining (≈ 0.05) for GW-7, suggesting intermediate flow before mining, and quick flow after mining. Sahu et al. (2009) suggested that a gain function less than 0.4 indicates strong attenuation of input signals or an aquifer with small to moderate storage

capacity. The observations can be interpreted as due to fractures that created more flow pathways during and after mining and caused faster flow.

The coherence function indicates whether the changes in the output series correspond to the same type of changes as the input signal. Figure 11a, b show variations in the coherence function for pre- and post-mining conditions, respectively. The coherence functions display different variations at different frequencies, which is consistent with the gain function, showing a similar pattern of attenuation and filtering of the input signal. In Fig. 11a, a high consistency was observed between the input (precipitation) and output (hydraulic heads) at frequencies 0.05–0.12, 0.2–0.25, and 0.48–0.5 before mining. In contrast, the peak of coherence function decreased for after mining (Fig. 11b) with higher values at frequencies 0.15–0.25, indicating less consistency between the input and output signals. The mine void space, which drains water from the upper aquifer, is a perturbation

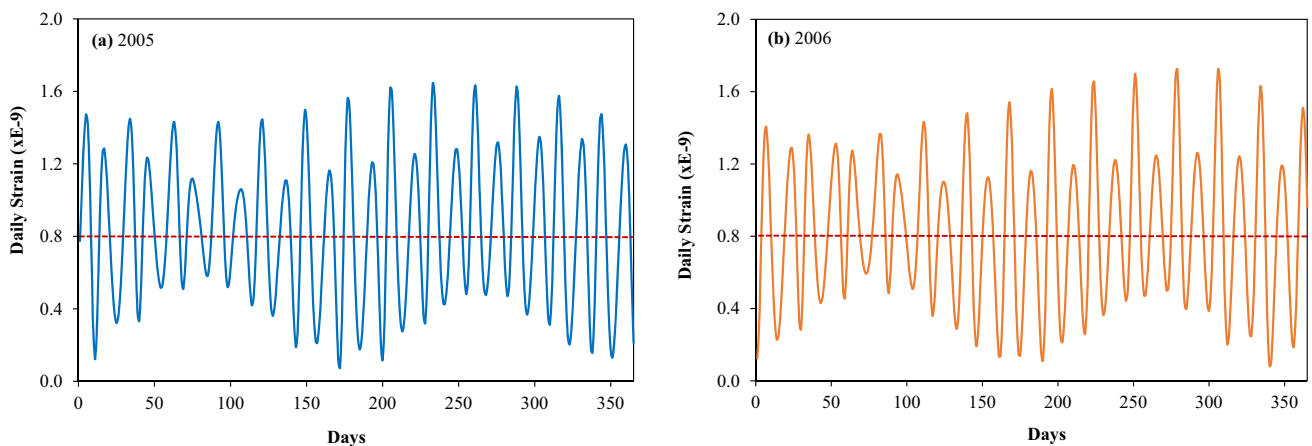


Fig. 12 Typical Earth-tide strain data **a** 2005; **b** 2006. Red dashed line is the average daily strain value for each year ($0.85\text{E}-9$)

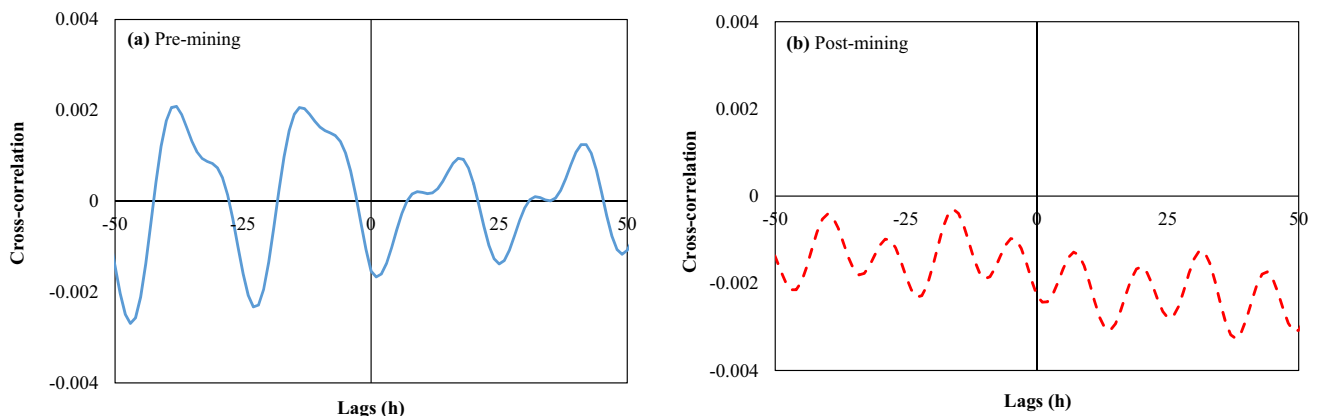


Fig. 13 Comparison of cross-correlation of daily Earth tides and hydraulic heads of GW-4: **a** pre-mining; **b** post-mining

that was not present before mining and explains the low coherence observed after mining.

Time Series of Earth Tides and Well Hydraulic Heads

Earth tide strain data for years 2005 and 2006 were plotted in Fig. 12, which display a monthly cyclic pattern. Cross-correlation analysis was conducted using hourly Earth tide strain as input and hydraulic heads as output. As shown in the cross-correlogram (Fig. 13a, b) for well GW-4, the maximum $r_{xy}(k)$ was less after mining and the cyclic pattern was not as prominent as before mining. These results indicated that the system had weaker responses to Earth tides after mining. Water draining to the underlying mine or new fractures can be an important process during and after mining, reducing the impacts of Earth tides as hydraulic heads responded to other more influential factors. This impact can also be seen in the cross-amplitude plots (Fig. 14a, b), where the cross-amplitude magnitude was slightly reduced after mining, especially for the 1/12 cycle (at the frequency of 0.1). These results indicate that the post-mining system effectively attenuated the input signal of Earth tides, and that it then vanished to zero (Fig. 14b).

Specific Storage and Porosity

According to Marsaud et al. (1993), the barometric efficiency (B) can be estimated using the value of the gain function at the frequency of the daily barometric variation. Four values were found from the cross-correlation of barometric pressure and hydraulic heads of GW-4 and GW-7 during pre- and post-mining conditions at the frequency of 0.041 cycles/h. The barometric efficiency values were 0.02 and 0.01 for GW-4 during pre- and post-mining conditions; and 0.05 and 0.04 for GW-7 during pre- and post-conditions,

respectively. Table 4 shows the results from specific storage and porosity calculations using Eqs. (1) and (2).

The estimated specific storage values were small, in the range of 10^{-7} . The low values were likely due to the short-term effects of the earth tides and barometric effects; their durations were probably not long enough for the smaller fractures responsible for storage to be involved when the flow was primarily transmitted through large, connected fractures. The results also suggest that the aquifers were unconfined because the effects of earth tides and barometric pressure are usually negligible in unconfined aquifers (Larocque et al. 1998). In addition, there was a decrease in the specific storage coefficient for post-mining conditions when compared to pre-mining conditions in both GW-4 and GW-7. This is consistent with the observation that mining can decrease the storage coefficient (Booth 2007), which probably reflects the increased fractures and drainage after mining. Thus, once the groundwater system has been disturbed by mining, its hydraulic properties will also be changed. Based on Eq. (2), the decreased storage coefficient will cause decreased porosity, which is true for an undisturbed porous medium. However, in this case, the lower storage coefficients were caused by the aquifer losing its capacity to hold water when new fractures were induced by mining, and these new fractures may not be accounted for due to the short-term effects of earth tides. Therefore,

Table 4 Specific storage and porosity from times series analyses

Parameters	GW-4		GW-7	
	Pre-mining	Post-mining	Pre-mining	Post-mining
Specific storage ($\frac{1}{m}$)	9.84×10^{-7}	7.03×10^{-7}	8.20×10^{-7}	7.77×10^{-7}
Porosity (%)	0.42	0.15	0.88	0.67

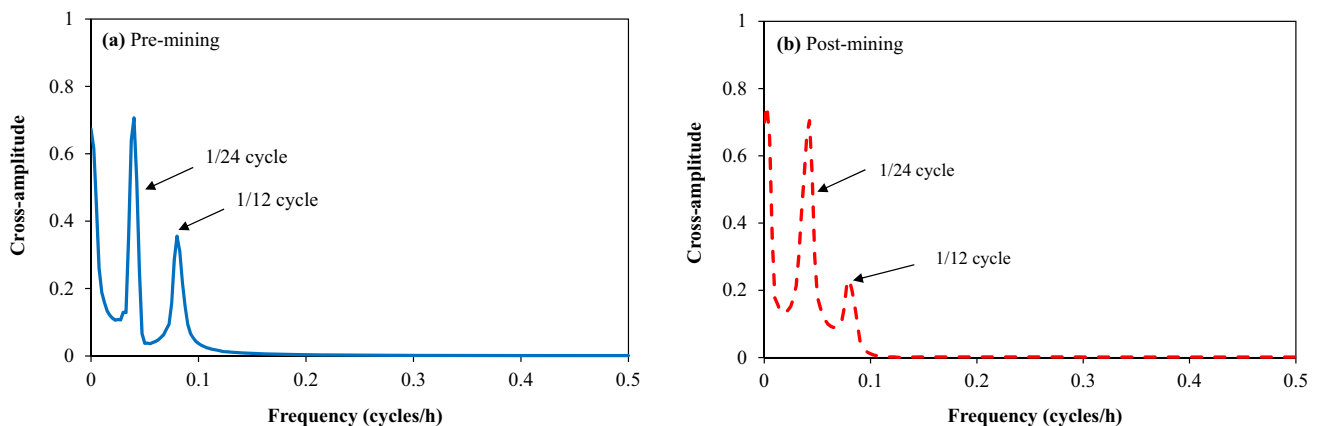


Fig. 14 Comparison of cross-amplitude of daily Earth tides and hydraulic heads of GW-4 **a** pre-mining; **b** post-mining

the calculated post-mining porosities may not reflect the true values.

Summary and Conclusions

We used classical time and frequency domain analysis to compare the hydrologic characteristics and temporal variations of aquifers associated with underground mining. The groundwater system was treated as a filter, which transforms the input signal (precipitation, hydraulic heads, Earth tide) to an output signal (hydraulic heads). The time series analyses of precipitation, hydraulic head, and earth tide data provided useful information regarding the impacts of underground mining on the unsaturated zone and upper aquifers below an old growth forest in southeastern Ohio. The major findings are:

1. Hydraulic head changes due to precipitation occurred approximately 3 days after the rainfall during the period from September 2004 to December 2009.
2. Autocorrelation of daily hydraulic heads of the monitoring well (GW-3) showed more of a delay before mining than afterwards, which was probably due to higher hydraulic conductivities and flow velocities in the mined system.
3. Cross-correlation of daily precipitation and hydraulic head suggested a higher maximum cross-correlation coefficient and shorter delay after mining. The stronger and faster response was likely caused by the increased hydraulic conductivity created by mining. The results were consistent with those calculated by Cook (2006, 2008), who also observed a dramatic increase in hydraulic conductivity. Moreover, cross-correlation among hydraulic heads of shallower and deeper wells also suggested that the deeper well was losing water to the underlying mine, even though water levels in the shallow wells were rising due to precipitation.
4. Results from hourly precipitation and hydraulic head cross-correlation analysis displayed similar patterns as those from daily data analysis, which confirmed that time series analysis is a reliable way to investigate changes in hydraulic properties of mined areas. A shorter delay, and a decreased gain and coherence function were observed in the post-mining cross-correlograms, indicating that the input signal (precipitation) was transferred faster through the system after mining than before mining. A quickflow component was also noted for post-mining conditions, compared an intermediate flow component for pre-mining periods. Quick flow usually occurs when water is discharged in a short time period due to a well-connected groundwater system.
5. Specific storage decreased after mining, which means that the aquifer's capacity to release groundwater had declined during the hydraulic head drop, probably caused by the fractures and drainage associated with mining activities. We should note that the calculated specific storage coefficient for post-mining conditions probably does not represent the real conditions due to the lack of confining characteristics in the system, since the confining pressure has been lost due to fracturing of rocks; the observed reduced impacts of Earth tides on barometric pressure and hydraulic heads (low cross-correlation coefficient in the cross-correlograms (Fig. 12) are an expected response (Fetter 2001). However, the cross-amplitude plots (Fig. 13) displayed small peaks at 12 and 24 h periods, which indicates the Earth tides may still have limited effects on groundwater levels.
6. Aquifers in the southeastern part of Ohio are usually hosted in sandstone layers. The cement in these rocks is usually composed of carbonate minerals (i.e. calcite, aragonite, and dolomite) and can dissolve in water (D. Kidder, personal communication, Jan 2010). New fractures in the surrounding rocks of the aquifer should increase water flow and lead to increased rock dissolution, enhancing even further the size of the fractures and amount of water flow. This process has likely affected the evolution of the water table in Dysart Woods and has probably further accelerated the aquifer-draining process.

This study has demonstrated that time series analysis can be used to characterize the impacts of underground mining on groundwater systems, allowing one to observe the hydrodynamic response of aquifers following longwall mining. The adverse impacts of mining on aquifers are significant, and include more connected fractures, higher hydraulic conductivities, and decreased water levels in the overlying strata. This study also provided evidence to support the statement by Cook (2008) that existing buffer zones are not enough to protect old growth forests from the negative impacts of underground mining. To protect the entire ecosystem, new regulations should consider the watershed boundaries and groundwater divides to maintain the groundwater flow system. The results of this study are likely applicable to many other similar systems worldwide. Mining impacts aquifers above or below mined areas, changes their hydraulic properties, and affects water supply.

Appendix 1: Summary Table of Time Series Analysis Equations (Bosch 1995; Box and Jenkins 1976; Padilla and Pulida-Larocque et al. 1998)

Function	Equation
<i>Auto-correlation</i>	
Auto-correlation coefficient $r(k)$	$r(k) = \frac{C(k)}{C(0)}$
Correlogram, $C(k)$	$C(k) = \frac{1}{n} \sum_{t=1}^{n-k} (x_t - \bar{x})(x_{t+k} - \bar{x})$
<i>Cross-correlation</i>	
Cross-correlation coefficient $r_{xy}(k)$	$r_{xy}(k) = \frac{C_{xy}(k)}{\sqrt{\sigma_x \sigma_y}}$
Cross-correlogram $C_{xy}(k)$	$C_{xy}(k) = \frac{1}{n} \sum_{t=1}^{n-k} (x_t - \bar{x})(y_{t+k} - \bar{y})$
Cross-spectral function $S_{xy}(f)$	$S_{xy}(f) = h_{xy}(f) - i \lambda_{xy}(f),$ $h_{xy}(f) = 2[r_{xy}(0) + \sum_{k=1}^m (r_{xy}(k) + r_{yx}(k))D(k) \cos(2\pi f k)] \text{ (cospectrum)}$ $\lambda_{xy}(f) = 2[r_{xy}(0) + \sum_{k=1}^m (r_{xy}(k) + r_{yx}(k))D(k) \sin(2\pi f k)] \text{ (quadrature spectrum)}$
Cross-amplitude function $ S_{xy}(f) $	$S_{xy}(f) = S_{xy}(f) e^{-i\theta_{xy}(f)}$ $\theta_{xy}(f) = \arctan\left[\frac{\lambda_{xy}(f)}{h_{xy}(f)}\right] \text{ (phase function)}$
Coherence function $CO_{xy}(f)$	$CO_{xy}(f) = \frac{S_{xy}(f)}{\sqrt{S_x(f)S_y(f)}}$
Gain function $g_{xy}(f)$	$g_{xy}(f) = \frac{S_{xy}(f)}{S_x(f)}$

σ_x and σ_y are the standard deviations for the time series, \bar{x} and \bar{y} are the means of the series x_t and y_t , respectively; $D(k)$ is a weighing function necessary to overcome bias in the coefficients of $h_{xy}(f)$ and $\lambda_{xy}(f)$

References

- Altun AA, Yilmaz I, Yildirim M (2010) A short review on the surficial impacts of underground mining. *Sci Res Essays* 5:3206–3212
- Anderson D (2001) Probable hydrologic consequences. Ohio Valley Coal Company, Moody and Associates Inc, Meadville
- Bell FG, Genske DD (2001) The influence of subsidence attributable to coal mining on the environment, development and restoration; some examples from western Europe and South Africa. *Environ Eng Geosci* 7:81–99
- Bernard S, Delay F (2008) Determination of porosity and storage capacity of a calcareous aquifer (France) by correlation and spectral analyses of time series. *Hydrogeol J* 16:1299–1309
- Booth CJ (2002) The effects of longwall coal mining on overlying aquifers. *Geol Soc* 198:17–45
- Booth CJ (2006) Groundwater as an environmental constraint of longwall mining. *Environ Geol* 49:796–803
- Booth CJ (2007) Confined-unconfined changes above longwall coal mining due to increase in fracture porosity. *Environ Eng Geosci* 4:355–367
- Box GEP, Jenkins GM (1976) Time series analysis: forecasting and control. Holden Day, San Francisco
- Bredenhoeft JD (1967) Response of well-aquifer systems to earth tides. *J Geophys Res* 72:3075–3087
- Burgess MH (2006) The biohydrology of dysart woods. MS Thesis, Environmental Studies Program, Ohio Univ, Athens
- Chatfield C (1980) The analysis of time series: an introduction, 2nd edn. Chapman and Hall, London
- Chatfield C (2000) Time-series forecasting. Chapman and Hall, London
- Cook SR (2006) Effects of coal mining on perched aquifers above active longwall and room-and-pillar mines near dysart woods. BS Thesis, Dept of Geological Science Ohio Univ, Athens
- Cook SR (2008) The hydrogeology of an old growth forest with implications for defining impact zones associated with underground mining. MS Thesis, Dept of Geological Sciences, Ohio Univ, Athens
- Crosbie RS, Binning P, Kalma JD (2005) A time series approach to inferring groundwater recharge using the water table fluctuation method. *Water Resour Res* 41:1–9
- Fan GW, Zhang DS (2015) Mechanisms of aquifer protection in underground coal mining. *Mine Water Environ* 34:95–104
- Fetter C (2001) Applied hydrogeology, 4th edn. Prentice-Hall Inc, Upper Saddle River, pp 42–44–81–89
- Freeze RA, Cherry JA (1979) Groundwater. Prentice Hall Inc, Englewood Cliffs
- Ground Water Associates, Inc (1991) Hydrogeological evaluation of longwall mining at the Powhatan No. 6 mine and the potential impact to Dysart Woods (Draft). Prepared for The National Water Well Assoc, Ground Water Associates, Inc, Westerville
- Hasenfus GJ, Johnson KL, Su DWH (1988) A hydrogeomechanical study of overburden aquifer response to longwall mining. In: Peng SS (ed) Proceedings of the 7th international conf on ground control in mining, Morgantown, pp 149–162
- Healy RW, Cook PG (2002) Using groundwater levels to estimate recharge. *Hydrogeol J* 10:91–109

- Heish PA, Bredehoeft JD, Farr JM (1987) Determination of aquifer transmissivity from Earth tide analysis. *Water Resour Res* 23:1824–1832
- Holt J, Craig P (1997) Effects of longwall mining on forested areas. Ohio Valley Coal Co, P-SQUARED Technologies Inc, Knoxville
- Jacob CE (1940) On the flow of water in an elastic artesian aquifer. *Trans Am Geophys Union* 21(2):574–586
- Karacan CÖ, Goodman GVR (2009) Hydraulic conductivity changes and influencing factors in longwall overburden determined by slug tests in gob gas ventholes. *Int J Rock Mech Min Sci* 46:1162–1174
- Kendall MG, Ord JK (1990) Time series, 3rd edn. Oxford University Press, New York City
- Kendorski FS (1993) Effect of high-extraction coal mining on surface and ground waters. In: Proceedings of the 12th conference on ground control in mining, West Virginia University, Morgantown
- Kim JM, Parizek RR, Elsworth D (1997) Evaluation of fully-coupled strata deformation and groundwater flow in response to longwall mining. *Int J Rock Mech Min Sci* 34:1187–1199
- Kim T, Lee KK, Ko KS, Chang HW (2000) Groundwater flow system inferred from hydraulic stresses and heads at an underground LPG storage cavern site. *J Hydrol* 236:165–184
- Larocque M, Mangin A, Razack M, Banton O (1998) Contribution of correlation and spectral analyses to the regional study of a large karst aquifer (Charente, France). *J Hydrol* 205:217–231
- Lee JY, Lee KK (2000) Use of hydrologic time series data for identification of recharge mechanism in a fractured bedrock aquifer system. *J Hydrol* 229:190–201
- Léonardi V, Gavrilenko P (2003) Hydrologic measurements in wells in the Aigion area (Corinth Gulf, Greece): preliminary results. *C R Geosci* 336:385–393
- Liu J, Elsworth D, Matetic RJ (1997) Evaluation of the post-mining groundwater regime following longwall mining. *Hydrol Process* 15:1945–1961
- Manga M (1999) On the timescales characterizing groundwater discharge at springs. *J Hydrol* 219:56–69
- Marine IW (1975) Water level fluctuations due to earth tides in a well pumping from slightly fractured crystalline rock. *Water Resour Res* 11:165–173
- Marino G (2003) Geotechnical analysis of coal mining and reclamation permit D-360-12-Dysart Woods. Prepared for Buckeye Forest Council, Marino Engineering Assoc Inc, Urbana
- Marsaud B, Mangin A, Bel F (1993) Estimation of physical characteristics of deep confined aquifers from barometric efficiency and Earth tides. *J Hydrol* 144:85–100
- Marschalko M, Yilmaz I, Bednarik M, Kubecka K (2012) Influence of underground mining activities on the slope deformation genesis: Doubrava Vrchovec, Doubrava Ujala and Staric case studies from Czech Republic. *Eng Geol* 147–148:37–51
- McCathy BC, Small CJ, Rubino DL (2001) Composition, structure and dynamics of Dysart Woods, an old-growth mixed mesophytic forest of southeastern Ohio. *For Ecol Manag* 140:193–213
- National Park Service (2004) Dysart Woods National Natural Landmark: National Park Service, US Dept of the Interior. http://www.nature.nps.gov/nnl/Registry/USA_Map/States/Ohio/NNL/DW/index.cfm. Accessed 28 Aug 2016
- ODNR (Ohio Dept of Natural Resources) (2005) GeoFacts, history of coal mining in Ohio. <http://ohiocoal.com/downloads/history-ohio-coal-mining.pdf>. Accessed 3 Sept 2018
- OVCC (2003) Anticipated effects of planned subsidence, Addendum to Page 29, Part 3, K (5) (a), Powhatan No. 6 Mine, Permit D-0360. Received: May 5, 2003. Alledonia
- Padilla A, Pulido-Bosch A (1995) Study of hydrographs of karstic aquifers by means of correlation and cross-spectral analysis. *J Hydrol* 168:73–89
- Rojstaczer S, Agnew DC (1989) The influence of formation material properties on the response of water levels in wells to earth tides and atmospheric loading. *J Geophys Res* 94:12403–12411
- Sahu P, López DL, Stoertz MW (2009) Using time series analysis of coal mine hydrographs to estimate mine storage, retention time and mine-pool interconnection. *Mine Water Environ* 28:194–205
- Schillig P (2005) A hydrostratigraphic model for pre-mining control in a deciduous old-growth forest: BS Thesis, Geological Science, Ohio Univ, Athens
- Singh MM, Kendorski FS (1981) Strata disturbance prediction for mining beneath surface water and waste impoundments. In: Proceedings of the 1st conference on ground control in mining, pp 76–89
- Singh R, Mandal P, Singh A, Kumar R, Maiti J, Ghosh A (2008) Upshot of strata movement during underground mining of a thick coal seam below hilly terrain. *Int J Rock Mech Min Sci* 45:29–46
- Stoner JD (1983) Probable hydrologic effects of subsurface mining. *Groundw Monit Remediat* 3:128–137
- Wenzel HG (1996) ETGTAB—a program to predict tidal accelerations. Geodetic Institute, Karlsruhe Univ. <http://www.bfo.geophys.uni-stuttgart.de/etgtab.html>. Accessed 6 Aug 2018
- Zhang Q (2010) Use of time-series analysis to evaluate the impacts of underground mining on hydrological properties of Dysart Woods, Ohio. Thesis, Ohio University